Title

OPTIMUM PROPORTIONAL CONTROL OF A BLENDING PROCESS USING IMPRECISE FEEDBACK INFORMATION

Authors

Taylor, Carl N.
Foss, Alan.

Publication Date

1964-02-07

UCRL-11295

University of California

Ernest O. Lawrence Radiation Laboratory

OPTIMUM PROPORTIONAL CONTROL OF A BLENDING PROCESS USING IMPRECISE FEEDBACK INFORMATION

Berkeley, California

DISCLAIMER

Research and Development

UCRL-11295

UC-37 Instruments
TID-4500 (24th Ed.)

UNIVERSITY OF CALIFORNIA

Lawrence Radiation Laboratory
Berkeley, California

AEC Contract No. W-7405-eng-48

OPTIMUM PROPORTIONAL CONTROL OF A BLENDING PROCESS USING IMPRECISE FEEDBACK INFORMATION

Carl N. Taylor and Alan Foss

February 17, 1964

Printed in USA. Price $1.25. Available from the
Office of Technical Services
U. S. Department of Commerce
Washington 25, D.C.

OPTIMUM PROPORTIONAL CONTROL OF A BLENDING PROCESS USING IMPRECISE FEEDBACK INFORMATION

Contents

Abstract v

I. Introduction 1

II. Calculation of Mean-Square Concentration Fluctuations in a Controlled Blending Process 3

A. Description of Feedback Loop. 5

B. Calculation of MSE by Method of Acrivos. 6

C. Operating Conditions. 10

III. Apparatus. 13

A. Blender 13

B. Choice of Operating Conditions 13

C. Noise Generators. 17

D. Low-Pass Filters. 18

E. Proportional Controller. 18

F. Experimental System 18

G. Experimental Procedure 22

IV. Calculation Procedure. 24

A. Determination of MSE from Experimental Data. . . . 24

B. Determination of Autocorrelation Decay Parameters . . 26

V. Results. 30

VI. Predictions of Process Performance. 34

VII. General Conclusions 38

Acknowledgments 39

Appendices

A. Sample Calculations 40

B. Summary of Experimental Results 45

C. Circuit Diagram of Low-Pass Filters 46

D. Nomenclature with Typical Dimensions 47

References 49

OPTIMUM PROPORTIONAL CONTROL OF A BLENDING PROCESS USING IMPRECISE FEEDBACK INFORMATION*

Carl N. Taylor and Alan Foss

Lawrence Radiation Laboratory
University of California
Berkeley, California

February 17, 1964

ABSTRACT

This experimental study verifies the applicability of Acrivos's analysis of linear processes to a randomly disturbed continuous liquid blender which blends water and a salt solution. The process is controlled by a simple proportional controller which is fed imprecise feedback information. Evaluation of process performance is based on the time-averaged value of the square of the concentration fluctuations of the blended stream. Calculation of the mean-square-concentration fluctuations by Acrivos' method shows the mean-square deviations to be a function of loop gain, the relative magnitude of the measurement error and the effluent concentration fluctuations at zero control, the relative-frequency content of the measurement error and the input disturbance signals, and natural damping-frequency characteristics of the blending process.

The predictions of process performance calculated by this method are verified by the experimental results, which show that the mean-square deviations cannot be reduced to zero, but rather a minimum value is obtained as the amount of control action is varied. This minimum results from the counteraction of the favorable effect of feedback of the concentration measurement and the undesirable effect of measurement error.

In general, use of proportional control in this type of problem would greatly improve process performance when measurement error

---

* Prepared by Carl N. Taylor as an M. S. thesis in the Department of Chemical Engineering.

is either small or high-frequency in nature. When the measurement error is large, proportional control is ineffective and other types of control action are recommended.

I. INTRODUCTION

The purpose of this work is to study the application of simple proportional control to a randomly disturbed continuous liquid-blending process from which only imprecise feedback information is available. This type of control problem is common in the chemical-process industries in which process upsets result from many unpredictable disturbances. In such situations, corrective action must be based on physical measurements often acknowledged to be in error due to improper sampling and localized process fluctuations.

The physical blending process investigated in this study consists of a stirred cylindrical vessel fed continuously by two streams, one of concentrated salt solution and one of water. The flow rate of the salt solution was varied randomly, and the flow rate of the water stream was governed by a feedback signal derived from measurement of the concentration of the effluent from the vessel. A random disturbance was purposely added to the concentration feedback signal to simulate error in concentration measurement.

Our evaluation of the performance of the proportional feedback control was based on the time-averaged value of the square of the concentration fluctuations of the blended stream, as is generally recommended.[13, 12, 4, 10, 14]

The theoretical predictions of the effectiveness of proportional control applied to this process are based on the premise (shown later to be essentially correct for our system) that the blending process is linear. These theoretical predictions are derived from an analysis by Acrivos,[1] who has studied the response of linear stagewise processes to randomly fluctuating inputs. Acrivos's analysis, described in detail in the next section, shows the mean-square error (MSE) of the product-concentration fluctuations to be dependent upon the "strength" and "frequency content" of both the random input disturbance and the measurement error. This study further shows that the MSE cannot be reduced to zero, but rather a minimum value of MSE is obtained as the amount of control action is varied. This minimum results from counteraction of the favorable effect of feedback of the concentration measurement and the undesirable effect of measurement error.

Our objective was to verify the applicability of Acrivos's linear (and somewhat idealized) analysis to an actual blending process that cannot be properly represented as a process occurring in the perfectly mixed vessel assumed by Acrivos. Specifically, we sought to verify experimentally the behavior of the MSE as process parameters were varied and to observe the minimum predicted by the analysis.

Physical verification of the theoretical analysis would also justify using the analysis to draw some generalized conclusions about the effectiveness of proportional control in this type of control situation. It was of special interest to predict the effect on MSE of the input disturbance and measurement error.

In this work, the method of calculating the MSE of the product concentration fluctuations is first developed and shown to apply to our experimental system. The considerations concerning the design and construction of the experimental apparatus are then reviewed, and an explanation of the approximate calculation procedures used in the analysis of the experimental data given. The experimental results are then presented and discussed.

Included in the appendices are sample calculations, a summary of experimental results, a sketch of a circuit diagram for low-pass filters, and a nomenclature list with typical dimensions.

II. CALCULATION OF MEAN-SQUARE CONCENTRATION FLUCTUATIONS IN A CONTROLLED BLENDING PROCESS

In this section, the physical blending process studied will be shown to be a linear first-order process. Calculation of the mean-square concentration fluctuations in such processes by the method of Acrivos[1] shows the mean-square deviations to be a function of four dimensionless parameters: K_L (loop gain), $\frac{a^2}{\frac{a^2\beta^2K_m{}^2}{1+\nu T_B}}$ (the ratio magnitude of the measurement error and the effluent concentration fluctuations at zero control), μ/ν (the ratio of the frequency content of the measurement error to the error to the input disturbance signal), and νT_B (a measure of the natural damping characteristics of the blending process).

A schematic diagram of the experimental system is given in Fig. 1. The changes in effluent concentration caused by the random variations in the flow of salt solution were detected by a conductivity cell wired as a leg of an ac bridge. To simulate measurement error, a random noise signal was added to the output from the bridge, and the combined signal was converted to a pneumatic signal that operates the water-control valve.

Linearity of the blender was verified by frequency-response tests conducted by varying the flow of salt solution sinusoidally. Results showed the blender to follow linear first-order-amplitude damping and phase shift over most of the frequencies of interest. Excessive phase lags noted at high frequencies were apparently caused by a mixing delay or dead time in the blender. The dead time of the blender, as estimated from the frequency-response data, did not amount to more than 1/25 of the residence time of the blender and did not alter the representation of the blender as a linear first-order process. These results serve to justify the linearizations made in the following material balances.

The material balance on salt is represented by the equation

$$\frac{d(Vx)}{dt} = sx_0 - Fx , \qquad (1)$$

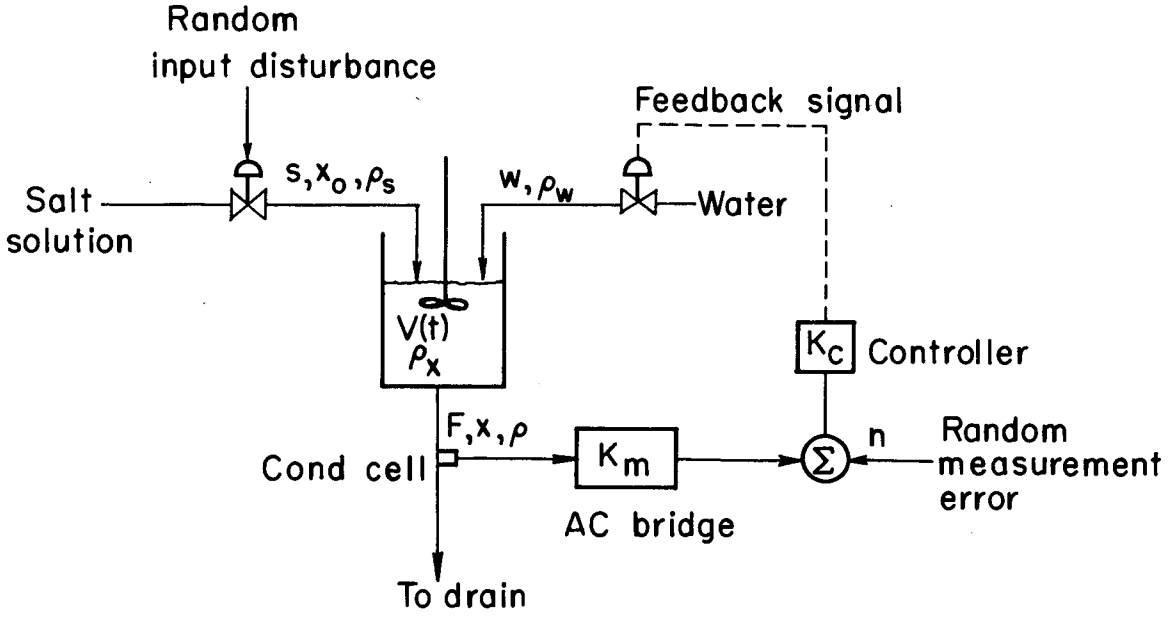

Fig. 1. Schematic diagram of experimental system for blending process.

and the total material balance is represented by

$$\frac{d(\rho V)}{dt} = s\rho_s + w\rho_w - F \,. \qquad (1a)$$

Since for the conditions of our experiments the density of our effluent stream was constant and our blending system was demonstrated to exhibit linear behavior, Eq. (1a) becomes

$$\frac{dV^*}{dt} = \frac{\rho_s s^*}{\rho} + \frac{\rho_w w^*}{\rho} - F^* , \qquad (2)$$

where (*) denotes deviations from steady state.

We substitute (2) into (1), linearizing (Vx) and remembering that the blender effluent rate is constant (i. e. $F^* = 0$). Equation (3) results:

$$\frac{dx^*}{d\theta} + x^* = a\, s^* + b\, w^* , \qquad (3)$$

where θ = dimensionless time = t/T_B

T_B = time constant of blender = $\frac{V_{ss}}{F}$,

ss = denotes steady state,

$$a = \left\{\frac{\partial x^*}{\partial s^*}\right\}_{ss} = \frac{1}{F}\left\{x_0 - \frac{x\rho_s}{\rho}\right\}_{ss},$$

and

$$b = \left\{\frac{\partial x^*}{\partial w^*}\right\}_{ss} = \left\{\frac{-x}{F}\,\frac{\rho_w}{\rho}\right\}_{ss}.$$

Although the parameters a and b can be evaluated from their definitions above, it was found more expedient to determine them experimentally by a simple calibration procedure prior to each run (see the sample calculations in Appendix A).

A. Description of Feedback Loop

The relation between perturbation in water-flow rate w^* and the elements in the feedback loop can be best seen in Fig. 1. The linear gain constants of the feedback amplifier (K_a), the electropneumatic transducer (K_T), the booster relay (K_B), and the water-control valve (K_v) were combined into one linear gain constant K_c. The linearity of these control elements was verified by frequency-response tests.

Use of the linear conversion constant K_m to represent the physical conversion of concentration fluctuations to electrical inpulses is done with the assumption that resistance varies linearly with concentration. This assumption of linearity is good within about 4% at the steady-state-product concentration (0.07 wt% NaCl) chosen for this experiment. We measured K_m experimentally by the simple calibration procedure outlined in Appendix A.

Thus, $w^* = K_c(K_m x^* + n^*)$ and Eq. (3) can be simplified to

$$\frac{dx^*}{d\theta} + Ax^* = z^*, \qquad (4)$$

where $A = 1 - bK_cK_m$ and

$$z^* = as^* + bK_cn^*.$$

Equation (4) shows that our entire physical system, including the blender and the feedback elements, can be described by a linear first-order process. The result of Acrivos's analysis of random fluctuations in such processes can now be applied directly.

B. Calculation of MSE by Method of Acrivos

For any linear process that can be described by an equation of the form of Eq. (4), Acrivos[1] shows that the MSE of effluent-concentration fluctuations can be related to the system parameters by

$$X_0 = \int_{-\infty}^{0} \exp A\tau \left[\int_{0}^{\infty} \exp(-Ay)\phi_{z^*z^*}(y)\, dy \right] \exp(A\tau)\, d\tau, \qquad (5)$$

where $\phi_{z^*z^*}$ = autocorrelation function of $z^*(t)$, and

X_0 = MSE of effluent-concentration fluctuations.

In his development Acrivos assumes that the random input disturbance and the random measurement error are stationary, i. e., the probability-density functions of these signals do not change with time. This was a valid assumption in our case because the probability-density functions of the outputs of the two noise generators used to create the input and measurement disturbances were guaranteed to be time invariant. We chose to use these two generators that produced

Gaussian noise because several investigators indicate that most random inputs encountered in the process industries can be considered Gaussian, at least as a first approximation.[1, 7, 11]

Except for the restriction just mentioned, Eq. (5) is applicable to multistage linear systems for which A, x^*, and z^* would represent large-order matrices. For our single-stage process, Eq. (5) simplifies to

$$X_0 = \int_{-\infty}^{0} \exp(2A\tau)d\tau \int_{\tau}^{\infty} e^{-Ay} \phi_{z^*z^*}(y)\, dy .$$

Integrating by parts, we obtain

$$X_0 = \frac{1}{2A} e^{2At} \int_{\tau}^{\infty} e^{-Ay} \phi_{z^*z^*}(y)\, dy \Bigg|_{-\infty}^{0} + \int_{-\infty}^{0} \frac{e^{2A\tau}}{2A} e^{-A\tau} \phi_{z^*z^*}(\tau)d\tau, \tag{5a}$$

$$X_0 = \frac{1}{2A}\int_{0}^{\infty} e^{-Ay} \phi_{z^*z^*}(y)\, dy + \frac{1}{2A} \int_{-\infty}^{0} e^{A\tau} \phi_{z^*z^*}(\tau)\, d\tau . \tag{5b}$$

Since the autocorrelation function is an even function,

$$\phi_{z^*z^*}(y) = \phi_{z^*z^*}(-y),$$

Eq. (5a) becomes

$$\boxed{X_0 = \frac{1}{A}\int_{0}^{\infty} e^{-Ay} \phi_{z^*z^*}(y)\, dy} . \tag{6}$$

To evaluate the integral in Eq. (6) it is necessary to determine $\phi_{z^*z^*}(y)$, the autocorrelation function of the combined input signal to the process.

By definition, $z^* = a s^* + b K_c n^*$.

By the familiar method of determining the autocorrelation function of a sum of two signals,[11] we obtain

$$\phi_{z^*z^*} = a^2 \phi_{s^*s^*} + b^2 K_c^{\,2} \phi_{n^*n^*} + \text{cross-correlation terms} .$$

Since our two signals are generated independently, the cross-correlation terms vanish.

As shown in Section III, the input and measurement-error signals were produced by filtering "white" noise with low-pass resistance-capacitance (RC) networks. The autocorrelation functions of our signals then had the form:[7, 11]

$$\phi_{s^*s^*} = \beta^2 e^{-\nu|t|},$$

$$\phi_{n^*n^*} = a^2 e^{-\mu|t|},$$

where β^2 and a^2 are the MSE or magnitudes of the signals and ν and μ are the decay parameters of the signals.

The integral in Eq. (6) can now be evaluated,

$$X_0 = \frac{1}{A} \int_0^\infty e^{-Ay} \phi_{z^*z^*}(y)\, dy. \qquad (6)$$

By substitution,

$$X_0 = \frac{1}{A} \int_0^\infty e^{-Ay} \left\{ a^2\beta^2 e^{-\nu T_B y} + b^2 K_c{}^2 a^2 e^{-\mu T_B y} \right\} dy,$$

and the solution

$$X_0 = \frac{1}{A} \left\{ \frac{a^2\beta^2}{A + \nu T_B} + \frac{b^2 K_c{}^2 a^2}{A + \mu T_B} \right\}$$

is obtained. Substituting the definition of A, we get

$$X_0 = \frac{1}{1 - bK_mK_c} \left\{ \frac{a^2\beta^2}{1 - bK_mK_c + \nu T_B} + \frac{b^2 K_c{}^2 a^2}{1 - bK_mK_c + \mu T_B} \right\}. \qquad (7)$$

Equation (7a), which takes into account the background noise (BGN) discovered in our system, was the equation actually used to evaluate the theoretically predicted values of MSE for the conditions of our experimental runs. Since our blending process was proven to exhibit linear first-order damping typical of a low-pass filter, we can assume that the process shapes the frequency spectrum of the supposedly random mixing disturbances to give an autocorrelation function of the form

$$\phi_{n^*n^*} = \gamma^2 e^{-\eta|t|},$$

where γ^2 = MSE of BGN in $(\text{volts})^2$, and

$\eta = \frac{1}{T_B}$ = reciprocal of time constant of blender.

Then the autocorrelation function of the combined process input becomes

$$\phi_{z^*z^*} = a^2\beta^2 e^{-\nu|\theta|} + b^2K_c^2\left\{\alpha^2 e^{-\mu|\theta|} + \gamma^2 e^{-\eta|\theta|}\right\}.$$

Thus,

$$X_0 = \frac{1}{1-bK_mK_c}\left\{\frac{a^2\beta^2}{1-bK_mK_c+\nu T_B} + \frac{b^2K_c^2\alpha^2}{1-bK_mK_c+\mu T_B} + \frac{b^2K_c^2\gamma^2}{1-bK_mK_c+\eta T_B}\right\}. \quad (7a)$$

As shown, the effect of BGN simply adds linearly to the input and measurement error terms. In all cases, the BGN term was an order of magnitude less than the other terms. For simplicity in the following discussion, Eq. (7) rather than (7a) will be considered to be the equation used to evaluate the theoretically predicted values of MSE for the conditions of our experimental runs.

To report our results on a more general basis, Eq. (7) was nondimensionalized by dividing the expression by the predicted MSE of conductivity fluctuations for the condition of zero feedback control. In so doing, loop gain K_L (a nondimensional measure of the level of proportional control) was introduced with three other dimensionless parameters. Equation (7b) was the result:

$$\frac{X_0}{\mathcal{X}_0} = \frac{1}{1+K_L}\left\{\frac{1+P_1}{1+K_L+P_1} + \frac{P_3K_L^2}{1+K_L+P_1P_2}\right\}, \quad (7b)$$

where $\mathcal{X}_0$ = MSE of concentration fluctuations for the condition of zero control $= \frac{a^2\beta^2}{1+\nu T_B}$,

K_L = loop gain $= -bK_mK_c$,

$P_1 = \nu T_B$,

$$P_2 = \frac{\mu}{\nu},$$

$$\text{and } P_3 = \frac{a^2}{\frac{a^2\beta^2 K_m{}^2}{1+\nu T_B}} = \frac{\text{magnitude of error signal}}{\text{magnitude of effluent concentration fluctuations at the condition of zero control}}.$$

Equation (7b) relates the dimensionless MSE of the effluent-concentration fluctuations to the dimensionless system parameters that represent the level of control and the magnitude and frequency characteristics of the process disturbance and the measurement error. Thus Eq. (7b) will predict process performance for a given set of system parameters. A typical plot of these theoretical predictions vs loop gain is shown in Fig. 2.

As Fig. 2 indicates, it is not possible to reduce the MSE to zero. Instead a minimum value of MSE exists for some optimum gain setting. Examination of Eq. (7b) shows that this minimum results from the favorable effect of feedback of the concentration signal (represented by the first term) and the undesirable effect of the measurement error (represented by the second term).

The purpose of our experimental study was to physically verify these theoretical predictions of process performance. In particular we sought to observe experimentally the predicted minimum and determine the accuracy with which this minimum was predicted.

C. Operating Conditions

The overwhelming task of data reduction limited the experimental investigations to three runs. The values of the process parameters for the three sets of operating conditions are listed below. During each experimental run, the actual fluctuations in product concentration were measured for eight or more values of loop gain ranging from about 0.5 to about 500.

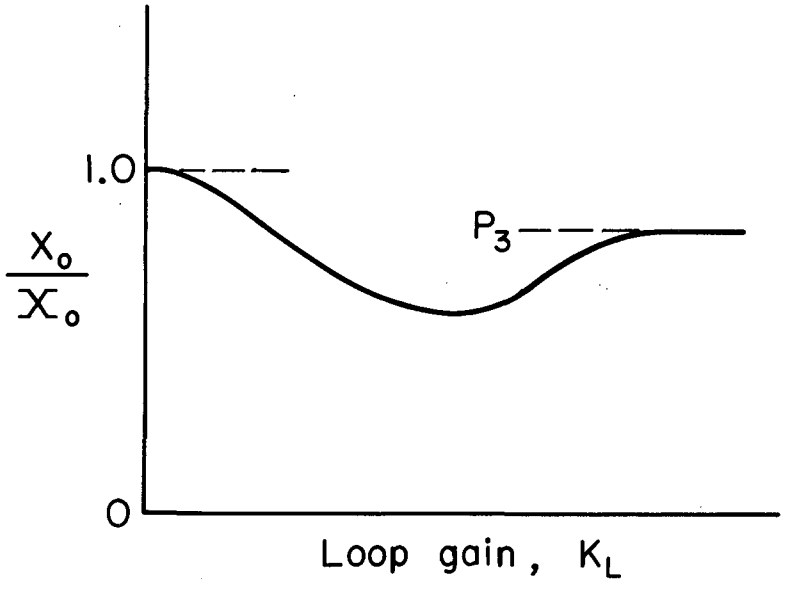

Fig. 2. Typical plot of process performance vs loop gain.

Operating Conditions

Run No.	T_B (sec)	P_3	Decay parameters (sec^{-1})	
			ν	μ
1	15	3.1	2.4	2.4
2	101	0.74	2.4	2.4
3	50	1.82	2.4	2.4*

* Because of lack of experimental data, an experimental value of μ could not be obtained for this filter setting. As a first approximation, it was assumed that $\mu = \nu = 2.4\ sec^{-1}$.

In the above table, T_B is the time constant of the blender, P_3 is the ratio of measurement-error signal to conductivity signal at zero gain, ν is the decay parameter of input disturbance and μ is the decay parameter of the measurement error.

A complete list of the values of the process parameters for the experimental conditions is given in Appendix B.

III. APPARATUS

The primary problem encountered in this study was to maintain linearity throughout the physical system. This section describes the limitations that this necessity for linearity placed on the design of our system.

A. Blender

A diagram of the blending vessel and mixing system is shown in Fig. 3. The configuration of the blender and impeller and the method of feed injection were changed until frequency-response tests conducted on the blender by sinusoidally varying the flow of salt solution indicated (see Fig. 4) that the system exhibited essentially linear frequency-response behavior according to sinusoidal damping of $\{1/[T_B(\omega)^2 + 1]\}^{1/2}$ and that the dead time of the blender had been minimized. The dead time of the blender, estimated from excessive phase lags noted at high frequencies, did not amount to more than 1/25 of the residence time of the blender for the conditions of our experiments. This small imperfection did not seriously alter the representation of the blender as a linear first-order process.

The vessel shown in Fig. 3 was made of Lucite to permit visual observation of the blending process. The vertical baffles were required to prevent formation of a vortex, and their final width (3/4 inch) is the result of a compromise between prevention of the vortex and minimization of mixing delay. The horizontal baffles were needed to prevent bubbles from forming at the air-water interface. These bubbles caused "blips" in the conductivity recording whenever one passed through the conductivity cell.

B. Choice of Operating Conditions

The steady-state concentration of the blended stream (0.07 wt% NaCl) was chosen because it falls on a nearly linear portion of the resistance-vs-concentration curve.[14] The maximum variation in the flow of salt solution was limited to ±20% so that the effluent concentration could not fall outside this portion of the curve within which the

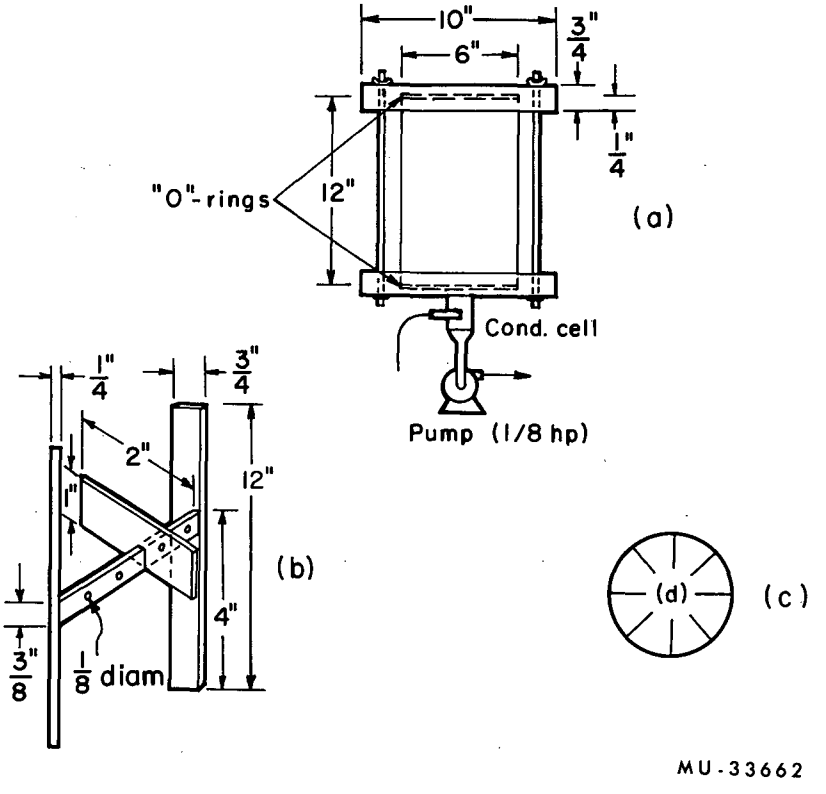

Fig. 3. Schematic diagram of blender and mixing systems (not to scale); (a) side view of blender used; (b) detail of baffle system showing two of the four vertical baffles and one of the eight horizontal baffles; (c) top view of horizontal baffles; (d) detail of feed injection and mixer system.

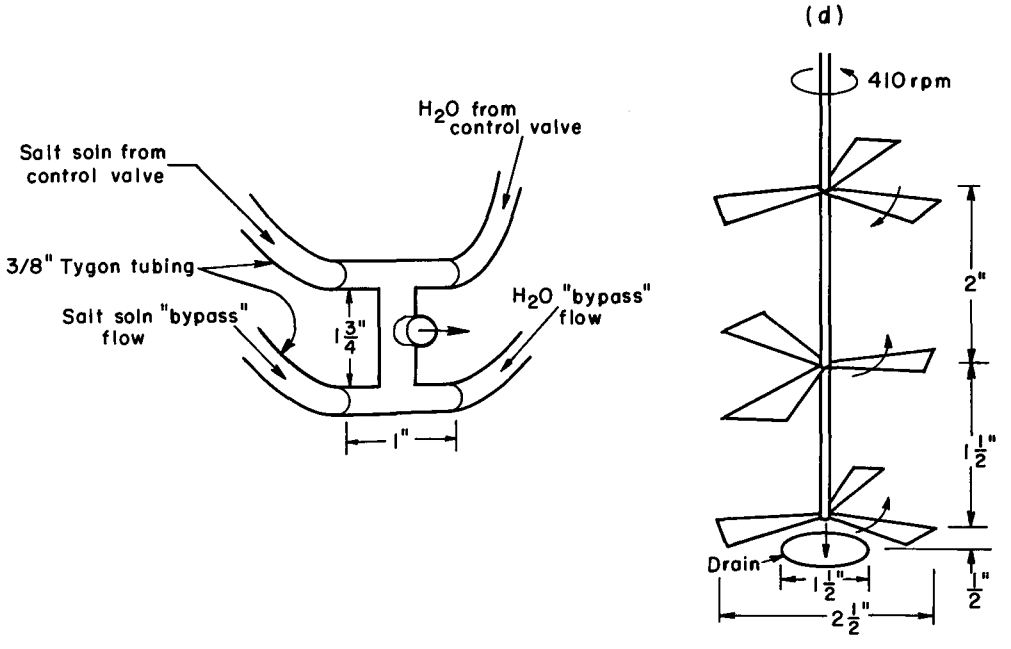

Fig. 3(contd.) (d) Detail of feed injection and mixer system.

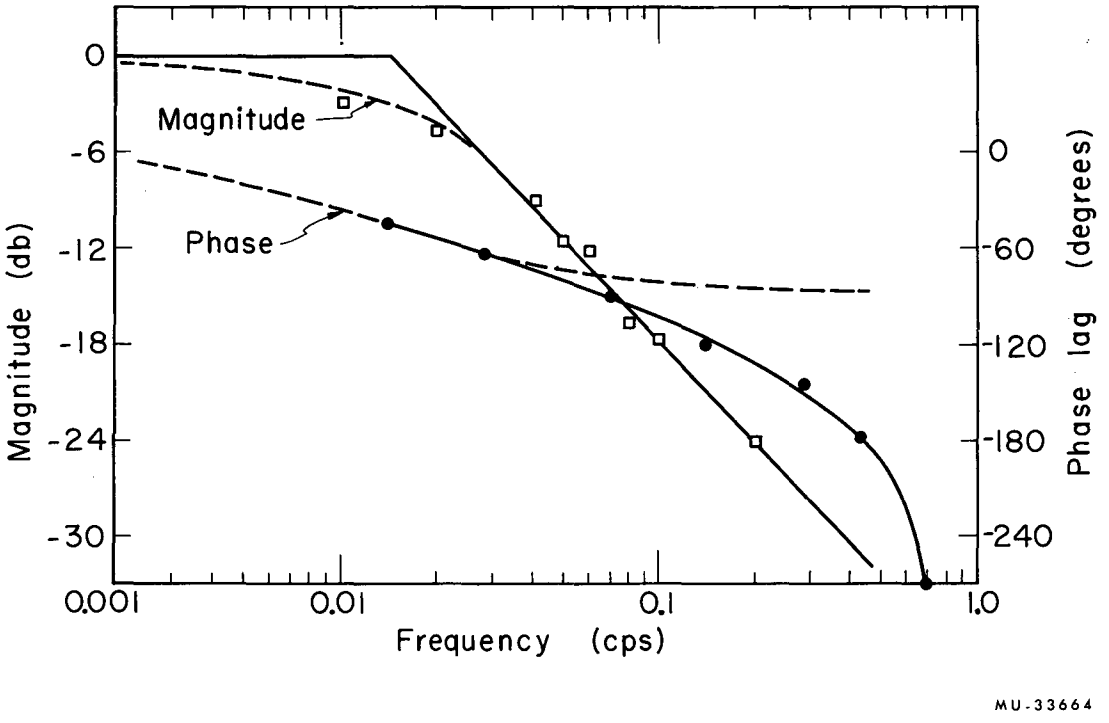

Fig. 4. Frequency response analysis of blender.

V = 0.5 gal
F = 2.6 gal/min
$\Big\rangle$ T_B = 11.5 sec

□ Experimental magnitude, O Experimental phase lag,
--- theoretical response of linear first-order blender.

assumption of linearity - - i.e., resistance = kx^* - - is valid within about 4 %.

The time constant of the blender was selected to be not less than 15 sec to insure that the dynamics of the blender dominated the entire system. The dynamics of the control valve and electropneumatic transducer were found to be inconsequential (up to a driving frequency of about 1 cps) compared with the dynamics of a blender having a time constant of 15 seconds or longer. The 15-second time constant also insured that concentration fluctuations of easily measurable magnitude were present in the frequency range of interest.

The volume of the blender and the steady-state flow rates were then chosen by compromise between considerations such as availability of equipment, drain capacity, and reliability of measurement. Once these basic design conditions were met, enough flexibility was built into the equipment to allow almost a decade variation in the flow rate, blender volume, and decay parameters of the input and measurement-error signals as shown below. The significance of these parameters is discussed shortly.

Process Parameter	Range
Steady-state flow rate	0.3 —3 gal/min
Blender-volume	0.25 —1 gal
Decay parameter of autocorrelation functions of random signals, ν and μ	0.628—6.28 sec^{-1}

C. Noise Generators

To duplicate typical process conditions in which the random input disturbance and the measurement error are completely unrelated, the random disturbance and the measurement error were generated by two independent noise generators. The noise generators used were nearly identical (Automation Laboratories, Low Frequency Gaussian Noise Generators, Model 100A) and had ± 15 V rms outputs. Their outputs were reported to follow a Gaussian distribution within 1% and have a "white noise" frequency spectrum that cuts off at 27 cps.

D. Low-Pass Filters

The low-pass filters placed on the outputs of the two noise generators served two purposes. The primary purpose was to shape the frequency spectrum of the random signals to the form $\beta^2\nu/(\nu^2+\omega^2)$ (shown in Fig. 5), which is typical of disturbances found in process streams.

The autocorrelation function of signals of this type is given by[7,11]

$$\beta^2 e^{-\nu|t|}.$$

The second purpose of the filters was to permit variation of the decay parameter ν. For the simple RC networks used (Fig. 6) ν is given by the reciprocal of the time constant of the network, in this case $1/RC$.

To maintain nearly constant output impedance of the filter and satisfy the electronic requirements of the feedback circuit, R remained fixed and C was made variable so that ν could be changed from 0.628 to 6.28 sec^{-1}. An upper limit of 6.28 sec^{-1} was set for ν by the limiting frequency-response characteristics of commercially available control valves.

The actual ν values of the filters were determined by frequency-response tests, and the results agreed with the design values. A detailed circuit diagram of the low-pass filters is given in Appendix C.

E. Proportional Controller

The proportional controller used in the experiment was a simple high-gain differential amplifier. The conductivity signal and the measurement error were added linearly in the amplifier, and the absolute gain of the combined signal could be varied continuously from 0.1 to 10. A simplified circuit diagram of the amplifier is shown in Fig. 7. Octal plug-in units manufactured by George A. Philbrick, Inc., were used in the amplifier as shown (K2-W and SK2-B).

F. Experimental System

A schematic diagram of the entire experimental system is given in Fig. 8. The salt solution was fed to the process from a pressurized

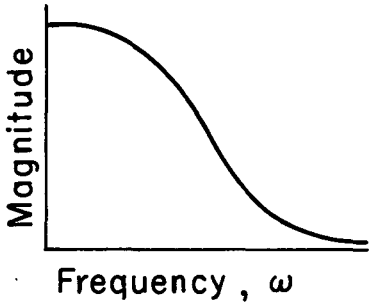

Fig. 5. Desired-frequency spectrum.

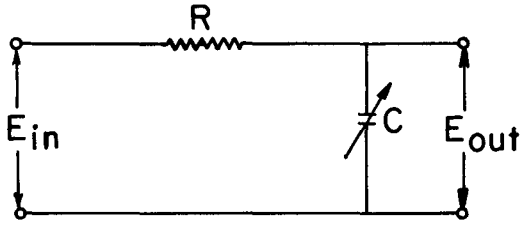

MU-33665

Fig. 6. Schematic diagram of low-pass filters.

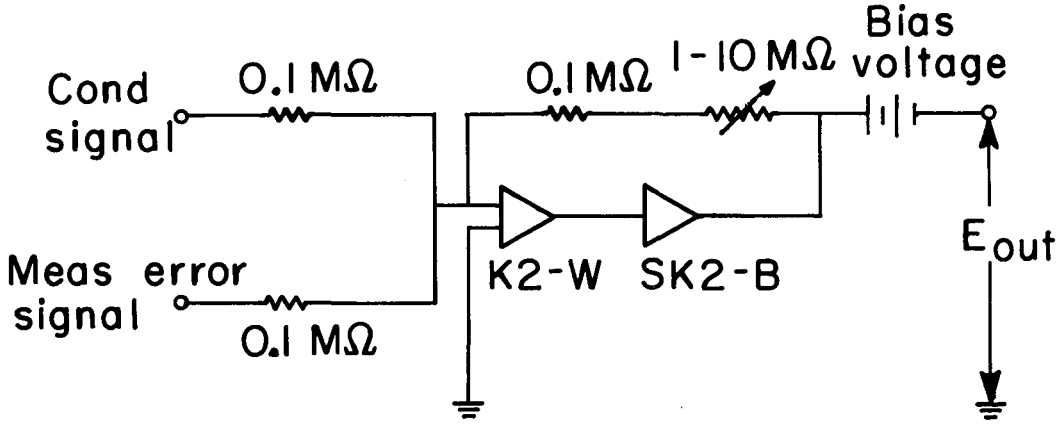

Fig. 7. Simplified circuit diagram of feedback amplifier.

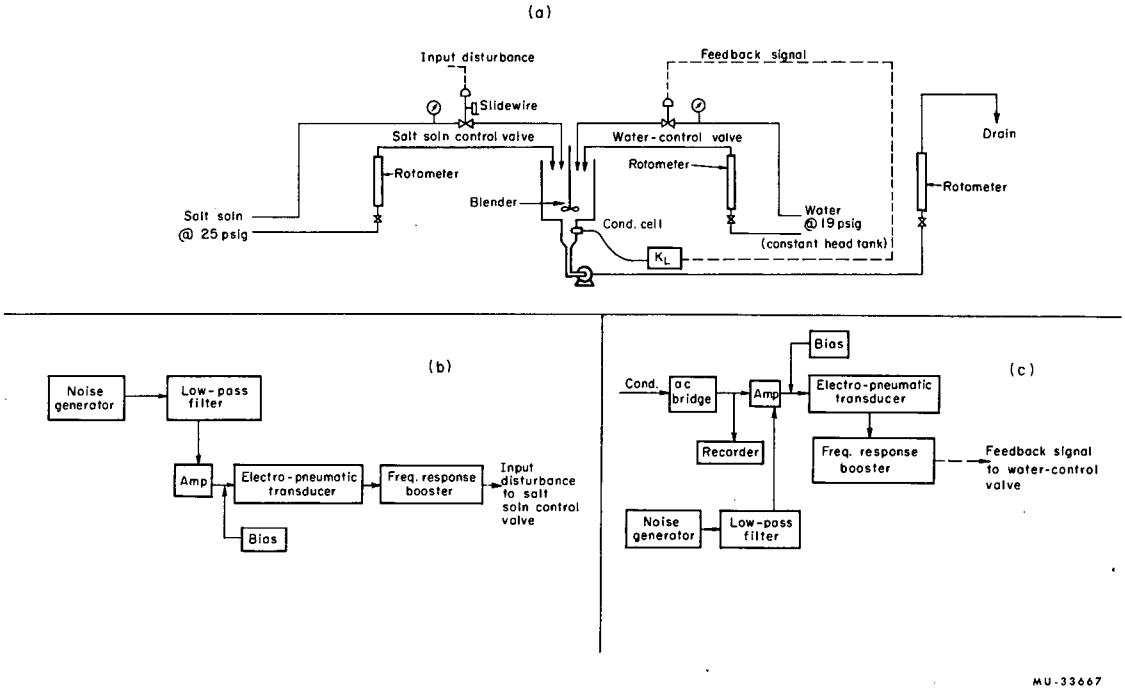

Fig. 8. (a) Schematic diagram of blending apparatus and related equipment; (b) detail of input disturbance; (c) detail of K_L.

tank maintained at 25 psig. The changes in effluent concentration created by random variations in the flow of salt solution were detected with a platinum conductivity cell wired as one leg of an ac bridge, and the combined signal was converted to a pneumatic signal. The pneumatic signal was passed through a pneumatic booster relay that operated the water-control valve. A constant-head tank was used as the water supply for the system.

Steady-state flows through the control valves were set by adjusting the bias voltage to the electropneumatic transducers, and the "bypass" flows into and out of the process were adjusted by manual control valves. The "bypass" flows could be adjusted to roughly 10 times the steady-state flows through the control valves. This permitted the total steady-state flows through the process to be varied by an order of magnitude (from 0.3 to 3 gpm) while the steady-state flows through the control valves remained unchanged.

The stirrer speed, set at 410 rpm, provided the best mixing without creating a great many bubbles at the air-liquid interface.

The random variation in flow of salt solution was determined from a recording of the stem position of the salt-solution control valve. The stem position was recorded by means of a resistance slide wire serving as a leg of an ac bridge.

G. Experimental Procedure

An experimental run was initiated by starting the steady-state flows through the blender at the predetermined rates. These steady-state flows were checked periodically during a run and adjusted as necessary. Once the flows had been adjusted properly and the level in the blender remained constant at the desired value, the stirrer was started and set at 410 rpm.

When steady state was attained, the sensitivity of the conductivity recording was reduced to minimize the effect of concentration fluctuations, and the ac bridge was balanced. This was the most important phase of experimental procedure, because a dc bias in the feedback signal resulting from an improperly balanced bridge would have changed

the steady-state flow of water through the process. The sensitivity of the conductivity recording was then increased, and the conductivity signal was recorded for the required 10 minutes.

The background noise was determined from a 10-minute recording of the conductivity signal taken with the feedback loop disconnected and with no input disturbances.

IV. CALCULATION PROCEDURE

This section describes the simple approximate procedures used to calculate the autocorrelation functions of the various random signals from experimental data. These approximate procedures could be used because the autocorrelation functions of these signals were known to be of the form $\beta^2 e^{-\nu|t|}$, and calculations were needed merely to estimate the value of the MSE (β^2) and the decay parameter (ν).

A. Determination of MSE from Experimental Data

The accuracy with which the MSE's of these random signals were determined was found to be dependent on the total sample length and sampling frequency chosen. Extending the total sample length and increasing the sampling frequency improved the accuracy of the determination, but this benefit had to be weighed against the clerical problem of analyzing overwhelming quantities of data.

Shannon's sampling theorem predicted that an interval of about 2.5 seconds or less between successive samples would be required to adequately describe these signals.[9] However, calculations of the MSE for a variety of sampling frequencies gave identical results when the interval between successive samples was 1 second or less. This sampling frequency of one sample per second was used in all subsequent calculations.

A moving average, often used in business forecasting,[3, 6, 8] was used in the calculation of MSE to compensate for slow drifts noted in the conductivity data. These drifts were attributable to hydraulic head variations in the water supply. The moving average is determined by calculating the mean values of successive "windows" of W seconds each as shown in Fig. 9. The MSE is then calculated from the expression given in Eq. (8):

$$\text{MSE} = \frac{1}{N'} \sum_{i=1}^{N'} (x_i - \mu_i)^2 , \qquad (8)$$

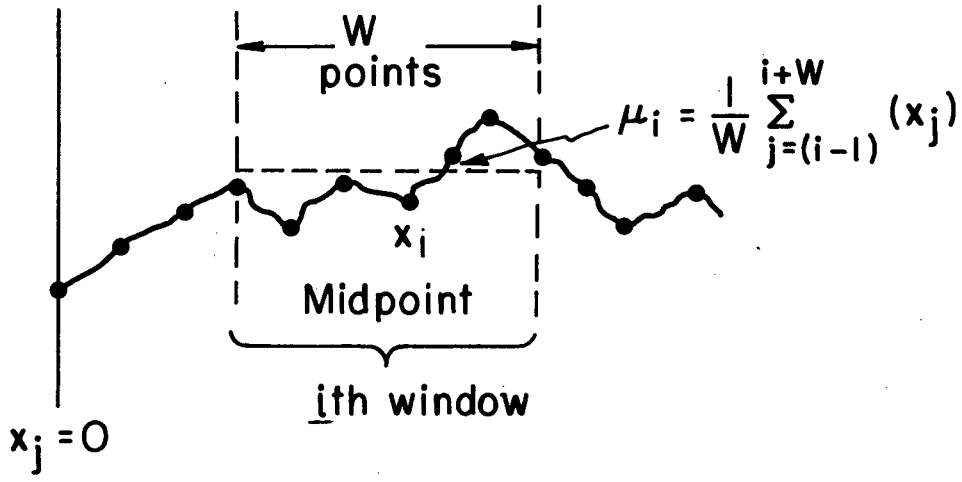

Fig. 9. Schematic diagram of determination of moving average.

where x_j = value of signal at jth sample point,

$j = 0, 1, 2, \cdots N$,

x_i = value of signal at midpoint of ith window,

$i = 1, 2, \cdots N - [(W/2) + 1]$,

$N' = N - [(W/2) + 1]$,

N = total number of samples taken = 600 at a frequency of one per second.

Calculations of the MSE of one of our concentration records (containing 600 data points) for a variety of window lengths W gave essentially identical results for window lengths ranging between 120 and 240 seconds as shown in Fig. 10. A window length of 240 seconds and a total sample length of 600 data points (10 minutes) were used to calculate the MSE of the conductivity fluctuations and the two random disturbances.

B. Determination of Autocorrelation Decay Parameters

The decay parameters ν and μ of the autocorrelation functions of the random signals were determined from records of the signals by the following approximate method.

For random signals that can be approximated by a series of step inputs, Chang recommends determining the decay parameters from experimental data by counting the number of step changes occurring during a given time interval.[6] The quantity ν is obtained by taking the limit as the time interval becomes large:

$$\nu = \lim_{T_{n+1} \to \infty} \frac{1}{T_{n+1} - T_n}, \qquad (9)$$

where 1 = number of step changes in time $(T_{n+1} - T_n)$.

As shown in Fig. 11, which is a portion of the recording of the stem position of the salt-solution-control valve, the random input disturbance could be approximated by a series of step changes.

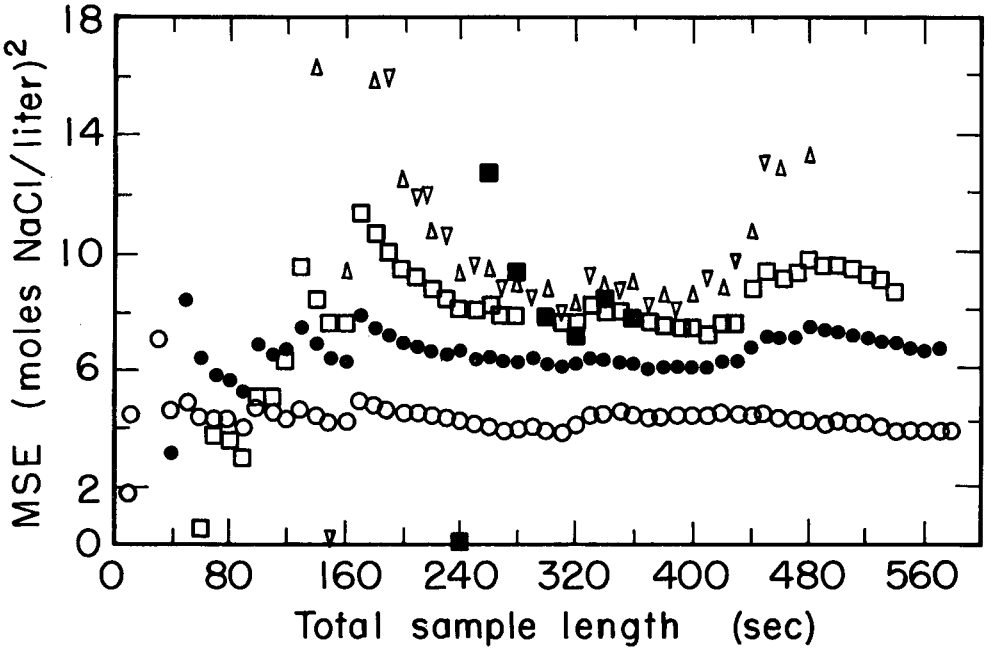

Fig. 10. MSE of conductivity signal calculated for various window lengths (W sec) (conductivity signal sampled at 1-second intervals).

Values of W in seconds: O, 30; ●, 60; □, 120; △, 240; ▽, 300; ■, 480.

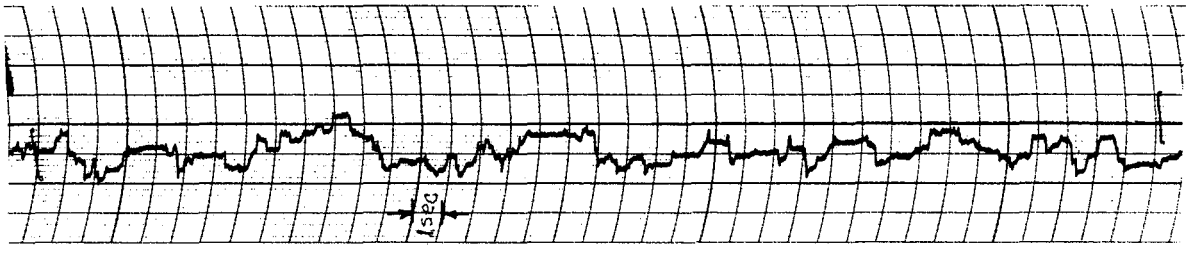

MU-33554

Fig. 11. Portion of actual oscillogram of stem position of salt-solution control valve.

Application of Eq. (9) to a 60-second section of the record yielded a ν value of 2.4 sec^{-1}, which is roughly five times the value calculated from the time constants of the low-pass filters.

Since the two random signals were generated by virtually identical noise generators and filtered by identical low-pass filters, it was assumed that the two decay parameters, μ and ν, were identical.

The discrepancy between the experimental and theoretical values of ν that we found is not unreasonable in view of the experience of other authors, who recommended that the autocorrelation function of random signals be evaluated experimentally whenever possible.[11]

V. RESULTS

The mean-square-concentration fluctuations, determined experimentally, are shown in Figs. 12 through 14 as a function of loop gain for blender time constants ranging from 15 to 100 seconds. The results are reported as a multiple of $\chi_0 = a^2\beta^2/(1+\nu T_B)$, the mean-square concentration fluctuation with no control.

In all cases, the experimental results exhibit the minimum in MSE, followed by the gradual deterioration in control as loop gain is increased. The experimental results compare favorably with behavior calculated [Eq. (7a)] from the linear analysis presented earlier.

Except for what appears to be a systematic error in one of the runs (Fig. 13), the experimental data deviate from Eq. (7a) in a consistent manner in all three cases. The scatter at low gain reflects the appreciable drifting of the steady-state conditions noted during the experiment. Drifts were believed to result from hydraulic head deviations in the water supply and line-voltage variation.

Experimental values of MSE larger than those predicted by theory at high values of loop gain were attributed both to the slight delayed mixing time noted in our blender and to possible phase lags in the electropneumatic transducer and water-control valve. In industrial installations, these and other phase lags will be present, meaning that the MSE can be expected to exceed that calculated by Eq. (7a) at high gains. In practice, the maximum tolerable gain is likely to be dictated by stability considerations that arise owing to these additional phase lags.

The generally good agreement between the experimental results and the theoretical predictions of process behavior lends support to the approximate methods of data treatment and the linear representation of a somewhat nonideal blending process. The theoretical development can then be used to make generalized predictions concerning the effectiveness of linear proportional control in this type of control problem when the process parameters are changed.

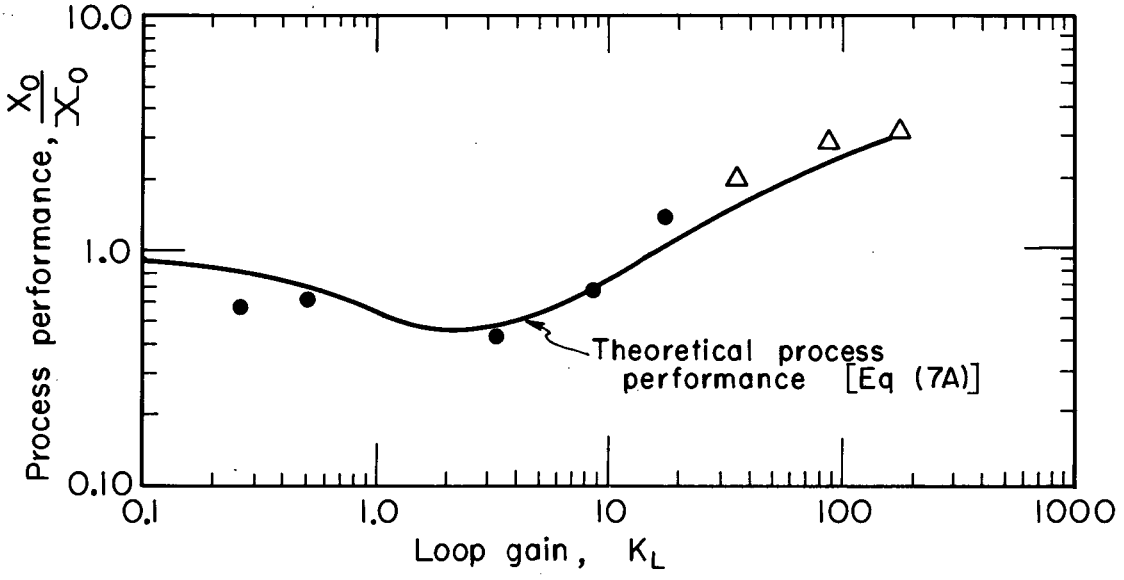

Fig. 12. Experimental results for Run No. 1 process performance vs loop gain. O, experimental measurements; Δ, experimental measurements corrected for limitations of amplifier.

$$\left.\begin{aligned} &\text{Flow} = 2 \text{ gal/min} \\ &V \quad = 0.5 \text{ gal} \end{aligned}\right\} T_B = 15 \text{ sec}$$

$$\nu = \mu = 2.4 \text{ sec}^{-1}$$

$$P_3 = \frac{(\alpha^2 + \gamma^2)}{\dfrac{a^2\beta^2 K_m^{\,2}}{1 + \nu T_B}} = 3.1$$

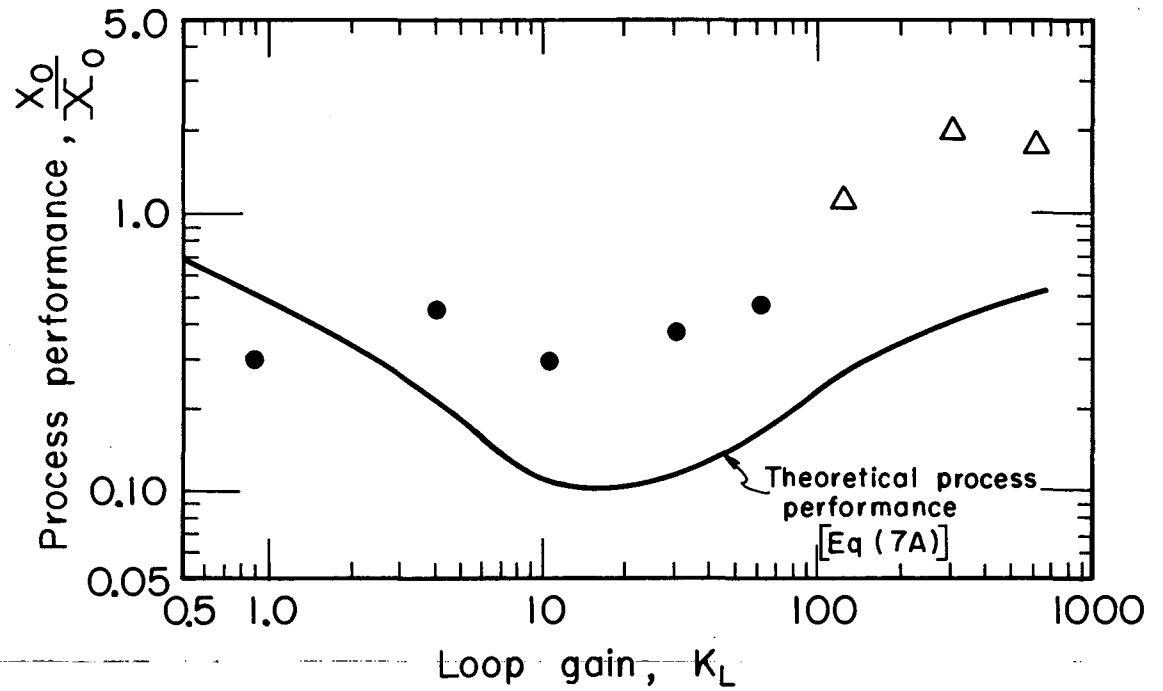

Fig. 13. Experimental results for Run No. 2 process performance vs loop gain. O, experimental measurements; Δ, experimental measurements corrected for limitations of amplifier.

$$\left.\begin{aligned} &\text{Flow} = 0.297 \text{ gal/min} \\ &V = 0.5 \text{ gal} \end{aligned}\right\rangle T_B = 101 \text{ sec}$$

$$\nu = \mu = 2.4 \text{ sec}^{-1}$$

$$P_3 = \frac{(\alpha^2 + \gamma^2)}{\dfrac{a^2\beta^2 K_m^{\,2}}{1 + \nu\, T_B}} = 0.74$$

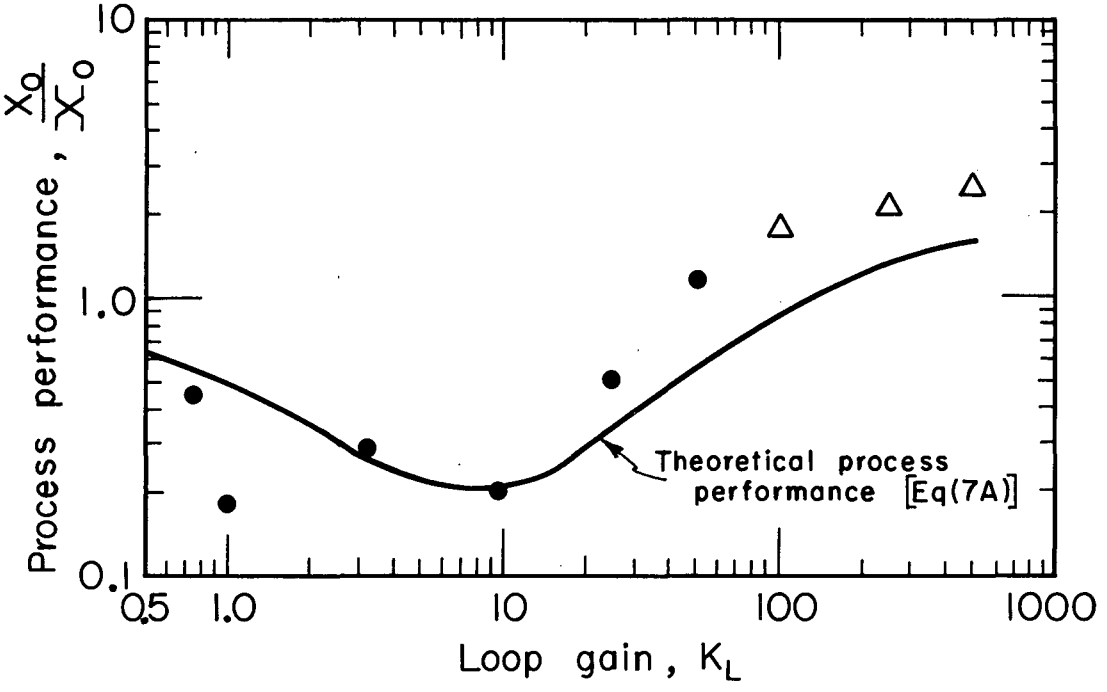

Fig. 14. Experimental results for Run No. 3 process performance vs loop gain. O, experimental measurements; Δ, experimental measurements corrected for limitations of amplifier.

$$\left.\begin{aligned} &\text{Flow} = 0.597 \text{ gal/min} \\ &V = 0.5 \text{ gal} \end{aligned}\right\rangle T_B = 50 \text{ sec}$$

$$\nu = \mu = 2.4 \text{ sec}^{-1}$$

$$P_3 = \frac{(a^2+\gamma^2)}{\dfrac{a^2\beta^2K_m^2}{1+\nu T_B}} = 1.82$$

VI. PREDICTIONS OF PROCESS PERFORMANCE

The performance of the blender-control system as calculated by Eq. (7b) over ranges of the four process parameters - - K_L, P_1, P_2, and P_3 - - is plotted in Figs. 15 and 16.

The effect of the magnitude of measurement error is down in Fig. 15. When there is no measurement error, the MSE of the product-concentration fluctuations can be reduced to zero by increasing the loop gain. This reduction of the MSE to zero cannot be realized in practice because of the error introduced at high values of loop gain by phase lags in the control elements. As shown, a minimum in MSE will normally by obtained as loop gain is increased. Note that when P_3 is small, the MSE can be markedly reduced by increasing loop gain, but that because of the shallow minimum there is little to be gained by searching for the optimum gain setting.

When the measurement error is large compared with the conductivity signal ($P_3 = 5$), there is only a slight reduction in MSE, and the MSE obtained at high values of loop gain is actually larger than the MSE for the condition of no control. In this situation there is no advantage to be gained by installation of the proportional controller.

Investigation of Eq. (7b) indicates that lengthening the time constant of the blender without reducing the magnitude of the measurement error would serve to further attenuate the effects of the input disturbance and will have the overall effect of increasing P_3, the ratio of the magnitude of the measurement error to the magnitude of the effluent-concentration fluctuations at zero control. The effect of increasing P_3 has already been demonstrated in Fig. 15.

Figure 16 shows the effect of the frequency content of measurement error on process performance. As expected, high-frequency measurement errors are tolerable because they are easily attenuated by the process, but low-frequency measurement errors reduce the effectiveness of proportional control. These results can probably be extrapolated to sampled-data-control systems in which the effects of measurement error upon sampling can be reduced by increasing the sampling frequency.

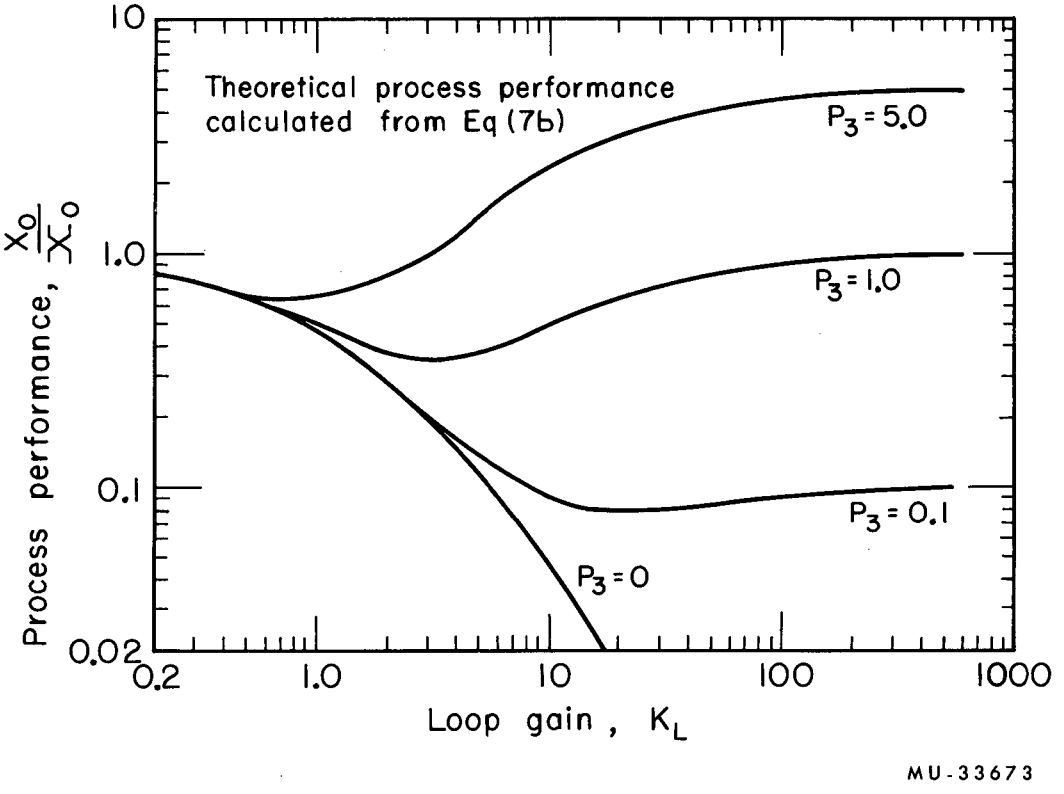

Fig. 15. Application of proportional control to a randomly disturbed liquid blender using imprecise feedback-information process performance vs loop gain for various values of P_3, the ratio of measurement error to concentration deviations at zero gain.

$$P_1 = \nu T_B = 0.189 \text{ sec}^{-1} \times 50 \text{ sec} = 9.5$$

$$P_2 = \left(\frac{\mu}{\nu}\right) = 1.0$$

$$\text{Process performance} = \frac{X_0}{X'_0} = \frac{1}{1+K_L}\left[\frac{1+P_1}{1+K_L+P_1} + \frac{P_3 K_L^2}{1+K_L+P_1 P_2}\right]$$

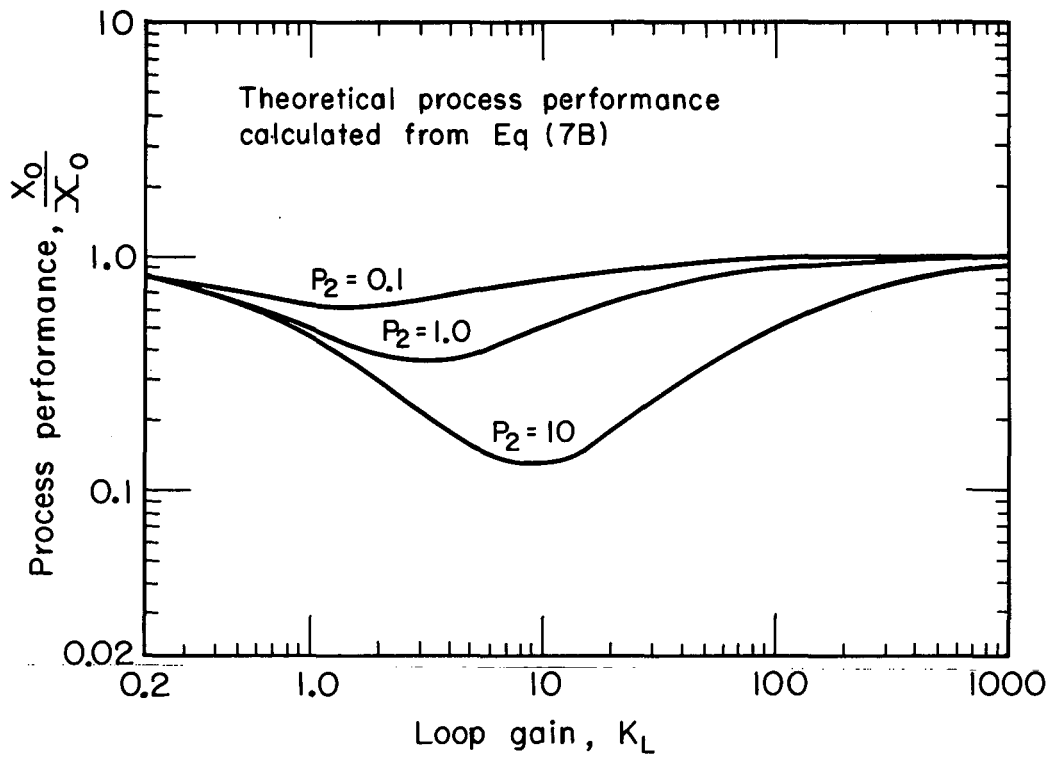

Fig. 16. Application of proportional control to a randomly disturbed liquid blender using imprecise feedback information process performance vs loop gain for various values of P_2, the ratio of frequency content of measurement error and input disturbance.

$$\nu T_B = 9.5,\ P_3 = 1.0,\ P_2 = \left(\frac{\mu}{\nu}\right)$$

$$\text{Process performance} = \frac{X_0}{\mathcal{X}_0} = \left[\frac{1+P_1}{1+K_L+P_1} + \frac{P_3 K_L^{\,2}}{1+K_L+P_1 P_2}\right]$$

Figure 16 also indicates that the value of MSE at high loop gain is independent of the decay parameter of the measurement error and is determined solely by its magnitude. In practice, however, the value of MSE at high loop gain will be larger than predicted because of phase lags in the control elements. Saturation of these control elements will prevent the MSE from increasing indefinitely at high loop gain and will determine the upper limit on MSE, just as saturation of the water-control valve placed an upper limit on the MSE of our experimental system.

VII. GENERAL CONCLUSIONS

Application of proportional control to this type of control problem would greatly improve process performance when measurement error is high-frequency in nature or when the magnitude of the measurement error is small compared with the magnitude of the effluent-concentration fluctuations. When the magnitude of the measurement error is large compared with the magnitude of the effluent-concentration fluctuations, the effectiveness of the proportional controller would be severely reduced.

In this situation, if the frequency content of the measurement error differs from that of the process output, the measurement error could be at least partially removed from the feedback signal by means of a narrow-band filter. This would improve the effectiveness of the proportional controller. Otherwise, a conceptually different kind of "filtering" is needed. One such controller extracts usable information from noisy signals by measuring and cross-correlating the process output with its manipulated input.[2]

ACKNOWLEDGMENTS

This work was made possible by a Research Assistantship granted by the U. S. Atomic Energy Commission. Thanks are due to the Kettering Foundation, whose grant in aid made computer time available, thus enabling us to complete the massive job of data reduction.

Many thanks go to the staff of technicians in the Department of Chemical Engineering and to students for assistance in constructing the equipment used in our investigations.

Thanks are also due to the Department of Electrical Engineering and the Department of Mechanical Engineering for the loan of equipment used in our experimental investigations.

APPENDICES

A. Sample Calculations

The first 10 calculations involved evaluating MSE from Eq. (10) for Run No. 1.

1. Determination of K_m

K_m is the conversion constant of the ac bridge and is measured by substituting a decade resistance for the conductivity cell and making a known change in resistance in the arm of the bridge:

$$K_m = \frac{\Delta \text{ output voltage from ac bridge}}{\Delta \text{ ohms}} = \frac{0.5 \text{ volt}}{10 \text{ ohms}}$$

$$K_m = \frac{0.05 \text{ volt}}{\text{ohm}} .$$

2. Evaluation of the Constants a and b

Both a and b were measured experimentally. With the process running unperturbed at steady state on open loop, a was evaluated by making a known change in the flow of salt solution and recording the change in output voltage from the ac bridge. Thus,

$$a = \frac{\Delta \text{ output voltage from bridge}}{\underset{\text{(measured experimentally)}}{\text{liters SS/sec}}} \times \frac{1}{K_m \text{ (volts from ac bridge)/ohm}}$$

$$a = \frac{1.48 \text{ V from bridge}}{\text{V to SSCV transducer}} \times 4.94 \times 10^3 \frac{\text{V to SSCVTr}}{\text{liters SS/sec}} \times \frac{20 \text{ ohms}}{\text{V from ac bridge}}$$

$$a = 1.46 \times 10^5 \frac{\text{ohms}}{\text{liters SS/sec}} = \left(\frac{\partial R^*}{\partial s^*} \right)_{ss} \text{ (for small perturbations).}$$

In the above equations, SS means salt solution, SSCVTr means salt-solution control valve transducer, and V means volts. We evaluated b similarly by making a known change in water-flow rate and recording the change in output voltage from the ac bridge.

$$b = \frac{-1.75 \text{ V from ac bridge}}{\underset{\text{(measured experimentally)}}{\text{V to WCV Tr}}} \times \frac{2.77 \times 10^2 \text{ V to WCV Tr} \times 20 \text{ ohms}}{\underset{\text{(from valve calibration data)}}{\text{V from ac bridge}}}$$

$$b = \frac{-9.7 \times 10^{3} \text{ ohms}}{\text{liters water per sec}} = \left(\frac{\partial R^{*}}{\partial w^{*}} \right)_{ss} \quad \text{(for small perturbations)}.$$

In the above equations, WCV means water-control valve.

3. Determination of β^2

The symbol β^2 represents the MSE of the variation of flow of salt solution into the process, as determined from a recording of the stem position of the salt-solution control valve. The stem position was indicated by means of a resistance slide wire serving as a leg of the ac bridge.

The slide wire was calibrated to yield

$$\frac{\text{V to SSCV Tr}}{\text{CLD on recording ac-bridge output}} = \frac{7.5 \text{ V to Tr}}{23.5 \text{ CL}} = \frac{0.319 \text{ V to Tr}}{\text{CL}}.$$

Then $\beta^2 = \text{MSE}(\text{CL})^2 \times \frac{\text{V to Tr}}{\text{CL}} \times \frac{\text{liters SS/sec}}{\text{V to Tr}}$

$$= 4.35(\text{CL})^2 \times \frac{0.319 \text{ V Tr}}{\text{CL}} \times \frac{2.02 \times 10^{-4} \text{ liters SS}}{\text{V to Tr}}$$

(from exptl data) (from value-calculation data)

$$\beta^2 = 1.81 \times 10^{-8} (\text{liters SS/sec})^2.$$

In these equations CL means chart line and CLD means chart-line deflection.

4. Determination of α^2

The symbol α^2 represents the MSE of the measurement-error signal recorded directly as a voltage signal:

$$\alpha^2 = 7.7 \times 10^{-2} (\text{volt})^2.$$

5. Determination of γ^2

The symbol γ^2 represents the MSE of the background noise (BGN) recorded as a voltage signal:

$$\gamma^2 = 3.48 \times 10^{-3} (\text{volt})^2.$$

6. Determination of ν

The decay parameters ν and μ are of the input disturbance and measurement errors, respectively:

$$\nu = \mu = \lim_{T_{n+1} \to \infty} \frac{1}{T_{n+1} - T_n},$$

where 1 = number of step changes in time $(T_{n+1} - T_n)$.

From experimental data, we know that $\nu = \mu = 2.4 \text{ sec}^{-1}$.

7. Determination of η

The symbol η is the decay parameter of the background noise.

Assume $$\eta = \frac{1 \text{ sec}^{-1}}{T_B}.$$

8. Determination of T_B

The symbol T_B is the time constant of the blender:

$$T_B = \frac{V}{F} = \frac{0.5 \text{ gal}}{2 \text{ gal/min}} = 0.25 \text{ min} = 15 \text{ sec}.$$

9. Determination of K_c

$$K_c = K_a \times K_T \times K_B \times K_v,$$

$$K_c = K_a \times 3.6 \times 10^{-3} \frac{\text{liter water/sec}}{\text{volt}} \text{ (from valve-calibration data)}.$$

For $K_a = 4.9$,

$$K_c = 1.77 \times 10^{-2} \frac{\text{liter water/sec}}{\text{volt}}.$$

10. Calculation of X_0

$$X_0 = \left\{ \frac{a^2\beta^2}{1-bK_mK_c+\nu T_B} \frac{b^2K_c^2a^2}{1-bK_mK_c+\mu T_B} + \frac{b^2K_c^2\gamma^2}{1-bK_mK_c+\eta T_B} \right\} \times \frac{1}{1-bK_mK_c}$$

$$bK_mK_c = \frac{-9.7\times10^3 \text{ ohms}}{\text{liters water/sec}} \times \frac{5\times10^{-2} \text{ volt}}{\text{ohm}} \times \frac{1.77\times10^{-2} \text{ liter water/sec}}{\text{volt}}$$

$$-bK_mK_c = +8.56 = K_L,$$

$$1 - bK_mK_c = 9.56,$$

$$\nu T_B = \mu T_B = 2.4 \text{ sec}^{-1} \times 15 \text{ sec} = 36,$$

$$\eta T_B = 1,$$

$$a^2\beta^2 = \frac{2.13\times10^{10} \text{ ohms}}{\text{liters SS/sec}} \times 1.81\times10^{-8} \text{ (liter SS/sec)}^2,$$

$$a^2\beta^2 = 3.86\times10^2 \text{ (ohms)}^2,$$

$$\mathcal{X}_0 = \frac{a^2\beta^2}{1+\nu T_B} = \frac{3.86\times10^2(\text{ohms})^2}{3.7\times10} = 10.4 \text{ (ohms)}^2,$$

$$b^2K_c^2a^2 = \frac{9.4\times10^7 \text{ ohms}}{\text{liters water/sec}} \times \frac{3.13\times10^{-4} \text{ liter water/sec} \times 7.7\times10^{-2}(\text{volt})^2}{\text{volt}},$$

$$b^2K_c^2\gamma^2 = 1.02\times10^2 \text{ (ohms)}^2,$$

$$X_0 = \frac{1}{9.56}\left\{ \frac{3.86\times10^2(\text{ohms})^2}{4.56\times10} + \frac{2.55\times10^3(\text{ohms})^2}{4.56\times10} + \frac{1.02\times10^2(\text{ohms})^2}{1.06\times10} \right\}$$

$$= \frac{1}{9.56}\left\{ 0.4 \text{ (ohm)}^2 + 5.67\times10 \text{ (ohms)}^2 + 9.62 \text{ (ohms)}^2 \right\}$$

$$X_0 = 7.28 \text{ (ohms)}^2$$

$$\boxed{\frac{X_0}{\mathcal{X}_0} = \frac{7.28 \text{ (ohms)}^2}{10.4 \text{ (ohms)}^2} = 0.691}$$

Theoretical prediction.

Our last calculations were made with experimental data at $K_a = 4.9$:

$$X_0 = MSE(CL)^2 \times \frac{\text{volts}}{CL} \times \frac{1}{K_m \text{ volts/ohm}}$$

(attenuator setting on recorder)

$$= 7.0(CL)^2 \times \frac{5 \times 10^{-2} \text{ V}}{CL} \times \frac{2 \times 10 \text{ ohms}}{\text{volt}}$$

$$X_0 = 7.0 \text{ (ohms)}^2$$

$$\boxed{\frac{X_0}{\overline{X}_0} = \frac{7.0 \text{ (ohms)}^2}{10.4 \text{ (ohms)}^2} = 0.674}$$

Experimental value.

B. Summary of Experimental Results

	Run No. 1		Run No. 2		Run No. 3	
Steady state flow through blender (gal/min)	2		0.297		0.597	
Volume of blender (gal)	0.5		0.5		0.5	
Blender time constant (sec)	15		101		50	
χ_0 = MSE at zero gain $(\text{ohms})^2$	10.4		42.0		26.4	
ν (sec^{-1})	2.4		2.4		2.4	
μ (sec^{-1})	2.4		2.4		2.4	
a (ohms/liter salt soln/sec)	1.46×10^{5}		7.5×10^{5}		4.2×10^{5}	
b (ohms/liter water/sec)	-9.7×10^{3}		-3.41×10^{4}		-2.77×10^{4}	
β^2 $(\text{liters salt soln/sec})^2$	1.81×10^{-8}		1.81×10^{-8}		1.81×10^{-8}	
α^2 $(\text{volts})^2$	7.7×10^{-2}		7.7×10^{-2}		7.7×10^{-2}	
γ^2 $(\text{volts})^2$	3.48×10^{-3}		5.2×10^{-4}		5.2×10^{-4}	
	K_L	$\frac{X_0}{\chi_0}$	K_L	$\frac{X_0}{\chi_0}$	K_L	$\frac{X_0}{\chi_0}$
	0.262	0.570	0.92	0.298	0.747	0.454
	0.507	0.608	4.12	0.453	0.997	0.182
	3.32	0.433	10.7	0.291	3.34	0.292
	8.57	0.674	30.1	0.377	9.47	0.201
	17.5	1.38	61.3	0.472	24.4	0.515
	35.0	1.94[a]	123	1.12[a]	49.8	1.15
	87.5	2.89[a]	307	2.02[a]	99.6	1.79[a]
	175.	3.14[a]	613	1.76[a]	249	2.16[a]
					498	2.5[a]

a. Experimental measurements corrected for limitations of amplifier.

The total experiment data consist of more than 15 000 individual data points and are not listed here.

C. Circuit Diagram of Low-Pass Filters

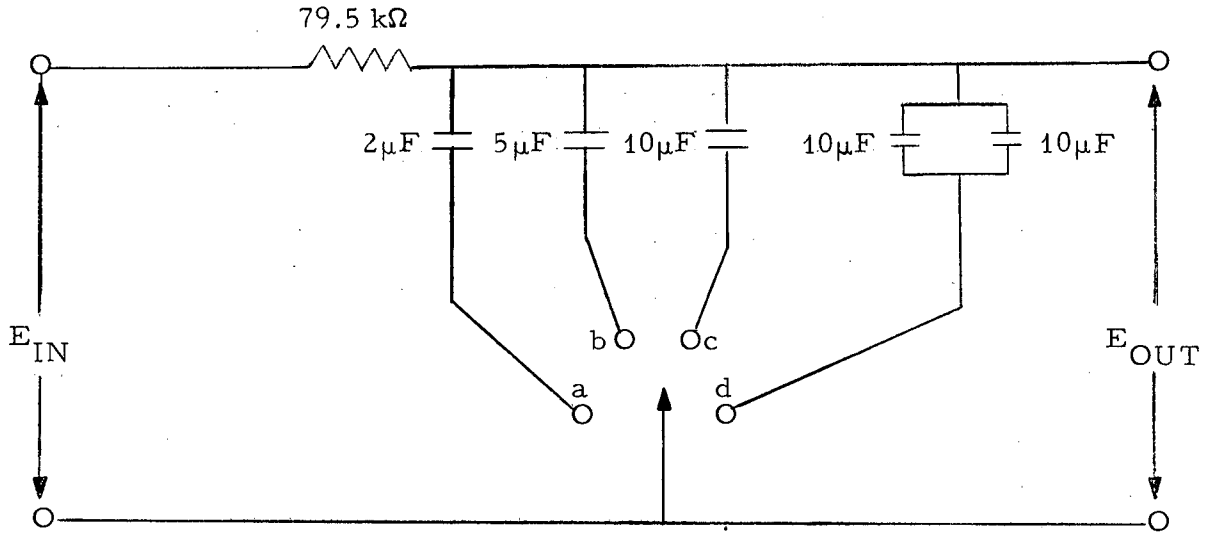

The resistance is a 2-watt 5% carbon resistor.

The capacitors are made of Pyranol with a 600-V dc breakdown voltage.

Summary of results of frequency-response tests on low-pass filters

	Break frequency of filter (cps)	
Filter setting	Filter #1	Filter #2
a	0.625	0.880
b	0.335	0.335
c	0.165	0.165
d	0.083	0.083

D. Nomenclature With Typical Dimensions

A = $[1 - bK_c K_m]$, dimensionless

a = $\left\{\frac{\partial x^*}{\partial s^*}\right\}_{ss} = \frac{1}{F}\left[x_0 - \frac{x\rho_s}{\rho}\right]_{ss}$, $\frac{\text{moles NaCl/liter}}{\text{liter salt soln/sec}}$

b = $\left\{\frac{\partial x^*}{\partial w^*}\right\}_{ss} = \left[-\frac{x}{F}\frac{\rho_w}{\rho}\right]_{ss}$, $\frac{\text{moles NaCl/liter}}{\text{liter water/sec}}$

F = total flow through blender, liter/sec

K_a = linear gain constant of feedback amplifier, dimensionless

K_B = linear gain constant of booster relay, dimensionless

K_c = $K_a K_B K_T K_v$, liters water per sec per volt

K_L = loop gain = $-bK_m K_c$, dimensionless

K_m = linear gain constant of ac bridge, volt/ohm

K_T = linear gain constant of electropneumatic transducer, dimensionless

K_v = linear gain constant of water-control valve, liters water per sec per volt

n = random disturbance added to feedback signal to simulate measurement error, in volts

P_1 = νT_B, dimensionless

P_2 = $\frac{\mu}{\nu}$, dimensionless

P_3 = $\frac{a^2}{\frac{a^2 \beta^2 K_m^2}{1 + \nu T_B}}$, dimensionless

R = resistance of effluent stream, in ohms

s = flow rate of salt solution, liters salt solution per sec

T_B = time constant of blender = V/F, in seconds

t = time, in seconds

V = volume of blender, in liters

w = flow rate of water, liters water per sec

x = concentration of blender effluent, moles NaCl per liter

X_0 = MSE of effluent-concentration fluctuations (moles NaCl per liter)^2

$\mathcal{X}_0$ = MSE of effluent concentration fluctuations under condition zero control, (moles NaCl per liter)^2

x_0 = concentration of salt solution, moles NaCl per liter

z = combined input concentration fluctuation, moles NaCl/liter

α^2 = MSE of measurement error, $(\text{volts})^2$

β^2 = MSE of input process disturbance, $(\text{liters salt soln/sec})^2$

γ^2 = MSE of background noise, $(\text{volts})^2$

η = decay parameter of background noise, sec^{-1}

θ = dimensionless time = t/T_B

μ = decay parameter of measurement error, sec^{-1}

ν = decay parameter of input process disturbance, sec^{-1}

ρ = density of effluent, g/liter

ρ_s = density of salt solution, g/liter

ρ_w = density of water, g/liter

ϕ = autocorrelation function, dimensionless

ω = frequency, sec^{-1}

subscripts

ss denotes steady-state values

superscripts

* denotes deviation variables

REFERENCES

1. A. Acrivos, Chem. Eng. Sci. 12, 279 (1960).
2. K. J. Astrom, R. W. Koercke, and F. Tung, On the Control of Linear Discrete Dynamic Systems with Quadratic Loss, IBM Research Dept. Report RJ-222, San Jose, Calif. (Sept., 1962).
3. Elmer C. Bratt, Business Cycles and Forecasting, (Richard Irvin Inc., Homewood, Illinois, 1953), Chapter 4.
4. Gordon S. Brown, and Donald P. Campbell, Principles of Servomechanisms, (John Wiley and Sons, New York, 1948).
5. Sheldon S. L. Chang, Synthesis of Optimum Control Systems, (McGraw-Hill, New York, 1961), Chapter 4.
6. Carl A. Dauten, Business Cycles and Forecasting, (South West Publishing Co., St. Louis, 1961), Chapter 10.
7. Wilbur B. Davenport, An Introduction to the Theory of Random Signals and Noise, (McGraw-Hill, New York, 1958), Chapters 4 through 6.
8. Griffith Evans, Mathematical Introduction to Economics, (McGraw-Hill, New York, 1930), Chapter 9.
9. Stanford Goldman, Information Theory, (Prentice-Hall, New York, 1953), Chapter 2.
10. E. M. Grabbe, Handbook of Automation, Computation, and Control, 3, (John Wiley and Sons, New York, 1958), Chapter 10.
11. G. C. Newton, L. A. Gold, and J. F. Kaiser, Analytical Design of Linear Feedback Systems, (John Wiley and Sons, New York, 1957), Chapters 3 through 5.
12. Rufus Oldenburger, Frequency Response, (McMillan Co., New York, 1956), Part IV.
13. John G. Truxal, Control Engineers Handbook, (McGraw-Hill, New York, 1958), Chapters 1 and 4.
14. John G. Truxal, Control System Synthesis, (McGraw-Hill, New York, 1955), Chapter 7.
15. International Critical Tables 6, 237, (McGraw-Hill, New York, 1933).